Bull. Mater. Sci., Vol. 39, No. 2, April 2016, pp. 559–567. © Indian Academy of Sciences.

Processing and characterization of screen printing $Ba_{0.5}Sr_{0.5}Co_{0.8}Fe_{0.2}O_{3-\delta}$ inks

MAGDALENA GROMADA[1], DAVIDE GARDINI[2,*], PIETRO GALIZIA[2] and CARMEN GALASSI[2]

[1]Institute of Power Engineering Ceramic Department CEREL, Research Institute, 1 Techniczna St., 36-040 Boguchwała, Poland

[2]National Research Council (CNR)—Institute of Science and Technology for Ceramics (ISTEC), Via Granarolo, 64-48018 Faenza (RA), Italy

MS received 5 March 2015; accepted 1 November 2015

Abstract. Oxygen-selective membranes based on thin layers of barium–strontium–cobalt ferrite $Ba_{0.5}Sr_{0.5}Co_{0.8}Fe_{0.2}O_{3-\delta}$ (BSCF) perovskite oxide were manufactured. Five BSCF inks prepared with different carriers and milling treatments were rheologically characterized, screen printed on three different porous alumina substrates and sintered at 1050 and 1150°C. The resulting membranes were characterized. The data collected on the rheological properties of inks (flow curves, thixotropic behaviour, linear viscoelasticity), their processability by screen printing, and the quality of the layers obtained after sintering represents an important starting point to set up the next research activities.

Keywords. Rheology; screen printing; perovskite-like material; oxygen membrane.

1. Introduction

The development of oxygen-selective membranes with a clear focus on reduced separation costs is desirable. Ceramic membranes for high-temperature oxygen separation with a mixed conductivity of oxygen ions and electrons were proposed more than 25 years ago by Teraoka *et al* [1]; in the subsequent years, intensive research was dedicated to the optimization of the composition in order to maximize the oxygen permeation and the stability. Barium–strontium–cobalt ferrite $Ba_{0.5}Sr_{0.5}Co_{0.8}Fe_{0.2}O_{3-\delta}$ (BSCF) perovskite oxide, largely employed for the fabrication of cathodes for solid oxide fuel cells (SOFCs), was found to be one of the most promising materials also for oxygen-selective membrane [2,3].

The oxygen permeation flux through membranes, in the range controlled by diffusion processes, is inversely proportional to the thickness of the membrane. It means that, in order to obtain the highest efficiency in oxygen separation, the thickness of membrane must be as low as possible. The limitation is the need to maintain an appropriate mechanical strength of the membrane. As a result, thin dense layers should be deposited on thick layers supports that it should be porous to facilitate the gas transport. In the literature, two approaches for manufacturing porous supports are presented. In the first, the support is fabricated starting from a perovskite-like material and a porous agent [4,5]. This solution protects the deposited thin layer of the membrane from cracking, during sintering because of the very similar shrinkage and coefficient of thermal expansion of support and dense layer material. In the second, more challenging case, the porous support is fabricated from alumina [6], magnesium oxide [7,8] or also metal [9], which ensure high mechanical strength.

In development of the thin membrane layers the setup of the screen printing inks plays an important role. However, in the literature only a few papers can be found regarding the rheological behaviour of inks for fabrication of appropriate layers in solid oxide fuel cells. In the paper of Somalu *et al* [10], the rheology of screen printing inks was described for the fabrication of porous composite anodes of nickel and scandia-stabilized zirconia. Somalu *et al* [11] also presented study of the effect of solid content on the rheological properties of anode screen printing ink. The rheological studies were performed using steady state, dynamic and creep-recovery tests. Screen printing pastes based on organic binder systems were developed by Ried *et al* [12] for the production of dense electrolyte layers of $Y_{0.16}Zr_{0.84}O_{1.92}$ (8YSZ) on Ni/YSZ anode substrates for anode-supported solid oxide fuel cells. The thixotropic behaviour of inks for screen printing method was analysed. Phair *et al* [13] investigated screen printing zirconia inks by rheological and imaging methods. The physical effects of binder composition on the topology, structure and thickness of the screen-printed layers were assessed by microscopy analysis.

In this paper, the focus is on the preparation and characterization of inks and the study of their performance during application by screen printing on alumina porous supports and after sintering at two different temperatures. The inks were rheologically characterized by measuring the flow curves (shear viscosity against shear rate), the

*Author for correspondence (davide.gardini@istec.cnr.it)

thixotropic behaviour which is important during levelling of the printed layer on the surface, and the viscoelastic properties (elastic G′ and viscous G″ moduli). The printed layers were observed by SEM and correlated with the rheological behaviour of the inks. The aim of this work is to investigate the effect of different formulations and methods of preparation (milling) on the properties of the screen-printed and sintered BSCF membranes.

2. Experimental

2.1 *Preparation of BSCF inks from perovskite powders*

Powder. $Ba_{0.5}Sr_{0.5}Co_{0.8}Fe_{0.2}O_{3-\delta}$ (BSCF) perovskite oxide powders were synthesized by solid state method. The BSCF perovskite powder was manufactured from the appropriate metal oxides: Co_2O_3 (minimal content of Co 70%, Sigma) and Fe_2O_3 (99% of purity, Sigma-Aldrich), and metal carbonates: $BaCO_3$ (99.5% of purity, Chempur) and $SrCO_3$ (99% of purity, Chempur). The raw materials were mixed with ethyl alcohol and milled for 2 h. The obtained powder was calcined in the electrical furnace for 5 h at 950°C. The process of milling and calcination was repeated three times to obtain monophasic material [14]. SEM images of the powder were collected with a FEI Quanta 200 ESEM^{TM} in low vacuum mode, while the XRD pattern was obtained with a Bruker D8 Advance in the range $10° \leq 2\theta \leq 80°$. Particle size distribution was determined through image analysis on 150 particles by dividing the grain size population in ten 1-μm wide bins. The specific surface area was measured by the low-temperature nitrogen adsorption method (77 K, Quantachrome Autosorb-1).

Carriers. Two different carriers, KF and KK, were prepared according to the compositions reported in table 1. The KF carrier uses terpineol (Merck KGaA) as dispersing medium, dioctyl phthalate (DOP) as dispersant (Merck KGaA) and ethyl cellulose with low molecular weight (5–15 mPa s of viscosity for a 5 wt% aqueous solution) as binder (Sigma-Aldrich). Instead, in the KK carrier, a mixture of two ethyl celluloses of different molecular weights (with viscosity of 5–15 and 30–60 mPa s for 5 wt% aqueous solution, Sigma-Aldrich) is used as binder and a proper thixotropic agent (Thixatrol, Elementies Specialties) was added to control the thixotropic properties. Both KF and KK carriers were prepared by heating the terpineol up to 50°C and then by adding the other additives under continuous mixing until the solution was clear.

Inks. Starting from the two carriers and the synthesized BSCF powders, five inks were prepared, differing in the powder content and milling treatment (table 2). The first two inks (BSCF KF (50.0%, PM) and BSCF KK (66.7%, PM)) were prepared by using a planetary mill with milling alumina pot of 500 ml and 50 alumina balls of diameter 10 mm and three balls of diameter 26 mm as milling media. The ratio between the mass of balls to the mass of BSCF suspension was equal to 13.6. The milling was set at a frequency of 250 rpm for 1 h. To make the inks more homogeneous and to reduce the presence of agglomerates, half volume of the two ball-milled inks was passed five times in a three-rolls mill (80 E, Exakt) by fixing a distance between the two couples of rolls of 15 μm and a rotating speed of 90 rpm and then five times more at 120 rpm by controlling the force with a distance between the rolls below 1 μm: BSCF KF (50.0%, PM + TRM) and BSCF KK (66.7%, PM + TRM). To study the effect of the

Table 1. Composition of the carriers.

Component	Function in carrier	KF composition (wt%)	KK composition (wt%)
Terpineol	Dispersing medium	73.2	78.0
Dioctyl phthalate	Dispersant	13.4	12.7
Ethyl cellulose (5–15 mPa s)	Binder	13.4	6.2
Ethyl cellulose (30–60 mPa s)	Binder	—	1.5
Thixatrol	Thixotropic agent	—	1.6

Table 2. Powder content and milling treatments for the inks.

Denotation	Carrier	Powder content (wt%)	Milling treatment
BSCF KF (50.0%, PM)	KF	50.0	Planetary mill
BSCF KK (66.7%, PM)	KK	66.7	Planetary mill
BSCF KF (50.0%, PM + TRM)	KF	50.0	Planetary mill + three-rolls mill
BSCF KK (66.7%, PM + TRM)	KK	66.7	Planetary mill + three-rolls mill
BSCF KF (66.7%, TRM)	KF	66.7	Three-rolls mill

additional three-rolls milling on the properties of inks, a fifth ink, containing the 66.7 wt% of BSCF powder in the KF carrier, BSCF KF (66.7%, TRM), was prepared by utilizing only the three-rolls mill according to the procedure described above. The stability/shelf life of such inks was proved to be longer than 2 months. After such period of time, a phase separation is observed but the inks can be rejuvenate and made ready for application again by slightly mixing. After 6 months some degradation was observed.

2.2 *Rheological characterization*

The rheological properties of carriers and inks were investigated by using a rotational rheometer (Bohlin C-VOR 120) equipped with a thermostatic unit (KTB 30). The tests were performed at 25°C by using parallel plates with rotor diameter of 20 mm and fixing 500 μm of gap between the plates (PP20). Flow curves in controlled rate mode between 0.063 and 63 s^{-1}, by considering 16 points in logarithmic scale with a time per point of 80 s, were obtained to determine the dependency of shear viscosity on shear rate. Such test was prolonged up to about 400 s^{-1} and then returned down till 0.063 s^{-1} to evaluate possible hysteresis and make comparisons with the data from thixotropic measurements. The thixotropic behaviour was tested by submitting the inks to shear rate jumps from a relatively high value (100 s^{-1}) down to lower values (10, 1, 0.1 and 0.01 s^{-1}) and by measuring the shear stress changes with time. The higher shear rates (100, 10 and 1 s^{-1}) were kept for 2 min, while the lower shear rates (0.1 and 0.01 s^{-1}) were kept for 4 and 8 min, respectively. This test allows to observe how the shear stress changes with time when structural changes occur in the samples. If irreversible phenomena do not occur, the changes can be fully ascribed to the thixotropy of the samples. The viscoelastic properties were measured in the linear viscoelastic region (LVER) by applying small stress amplitude oscillatory tests at constant strain in the frequency range 0.1–10 Hz. The linear viscoelastic region was previously found with oscillatory stress sweep tests from low (1 Pa) to high (1000 Pa) stress values at two different frequencies (0.1 and 10 Hz). The viscoelastic spectra are related with the microstructure of the samples and give information about the structuring.

2.3 *Preparation and characterization of the porous supports*

Sixty pre-sintered alumina supports from three ready for press powders (9922, 9922I and 9916F from Nabaltec)—20 samples for each body—were produced. The granulate powders were uniaxially pressed at 9 MPa into a mould of inner diameter of 34.5 mm and further compacted by isostatic pressing at 150 MPa. The green bodies were pre-sintered in an electrical furnace at 1000°C for 1 h according to the following thermal cycle: (i) from 20 to 1000°C in 10 h (about 100°C h^{-1}); (ii) kept at 1000°C for 1 h; (iii) from 1000 to 800°C in 2 h (100°C h^{-1}) and (iv) free cooling from 800°C. The pre-sintering curve was designed to get supports of apparent porosity of at least 40%, but maintaining enough mechanical strength and appropriate level of shrinkage. After pre-sintering, the diameter of 9922 and 9916F supports were 33.96 mm, while that of the 9922I support was 33.70 mm. The thickness of each support was 2.10 mm. After pre-sintering, the supports were ground with abrasive papers of gradation 600.

Table 3. Apparent density, water absorbability and apparent porosity of alumina supports.

Support	Apparent density (g cm^{-3})	Water absorbability (%)	Apparent porosity (%)
9922	2.31	17.96	41.49
9922I	2.27	18.54	42.17
9916F	2.25	18.88	42.57

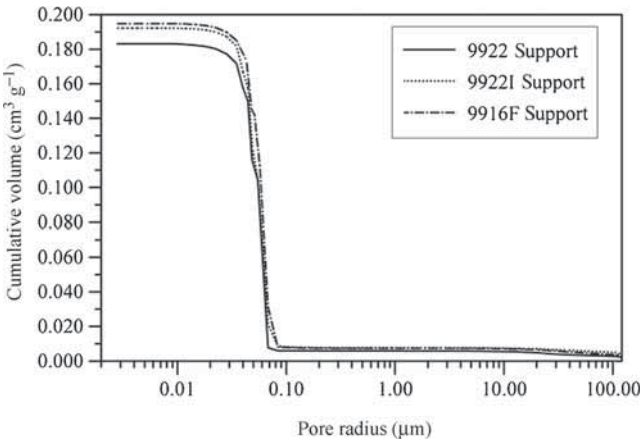

Figure 1. Distribution of pore-opening radii in alumina supports.

The basic properties of pre-sintered supports as apparent density, water absorbability and apparent porosity were estimated by Archimedes' method and boiling of samples impregnated with water (table 3).

The obtained values of apparent porosity ensure good access of air through supports to the dense membrane layer. The pore-size distribution was determined by mercury porosimetry (Micromeritics AUTO_PORE 4, model 9500). All the supports show comparable distributions of the pore-opening radii (figure 1). They are characterized by a quite narrow pore-size distribution ranging between 0.05 and 0.10 μm with a mean radius of 0.08 μm.

2.4 *Screen printing of thin perovskite layers on porous supports*

The deposition of the inks on porous supports was made with a semi-industrial screen printing machine (AUR'EL 900). The image on the screen (number of mesh 250) was a central circle with a diameter of 31 mm. A cardboard mask with a thickness slightly thinner than the support was prepared and fixed to the table of the screen printer. The distance between sample and screen (snap-off) was set at 900 μm. The forward

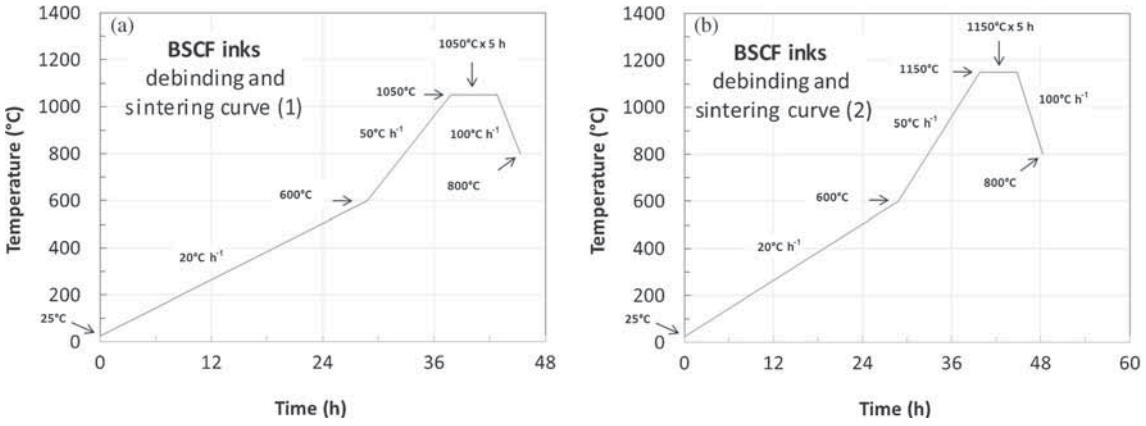

Figure 2. Debinding and sintering curves at (**a**) 1050 and (**b**) 1150°C.

and backward speeds of the squeegees were set at 80 mm s^{-1} and the applied force on the screen was fixed at 2.0 kgf.

The five inks were screen printed on four pieces of each support (9922, 9922I and 9916F), so that in total 60 samples were produced. As a membrane of approximately 20 μm thickness was desired, three passages of squeegee were set (thickness of a layer deposited by one passage estimated in about 5–10 μm). The first two passages were applied as forward and backward routes, while the third passage was performed after drying at 40°C for one night.

2.5 *Design of sintering curves*

The sintering curves were designed to get defect-free membranes adherent with the supports. The 60 samples of thin BSCF layer on alumina porous supports were equally divided into two groups. The first one was sintered at 1050°C for 5 h, while the second group was sintered at 1150°C for 5 h. Before sintering, both batches were subjected to a slow debinding cycle of 30 h (figure 2a, b). The densities of membranes were tested using a red dye penetrant BDR (Diffutherm) and by observing the degree of penetration through the samples.

3. Results and discussion

3.1 *Characterization of BSCF powder*

Particle size distribution of the synthesized BSCF powder ranges from submicron size to 10 μm with a mean particle size of 3.2 μm as shown by the analysis of SEM images on the powders (figure 3) and, according to, the specific surface area is small (1.1 m^2 g^{-1}). Moreover, the measurements of low-temperature nitrogen sorption showed that the BSCF powder exhibited only trace porosity (0.001 cm^3 g^{-1} [14]), which is an insignificant value of pores volumes per unit mass of sample. X-ray diffraction (XRD) pattern on the synthesized powders shows that cubic perovskite phase of $Ba_{0.5}Sr_{0.5}Co_{0.8}Fe_{0.2}O_{3-\delta}$ is formed (figure 4).

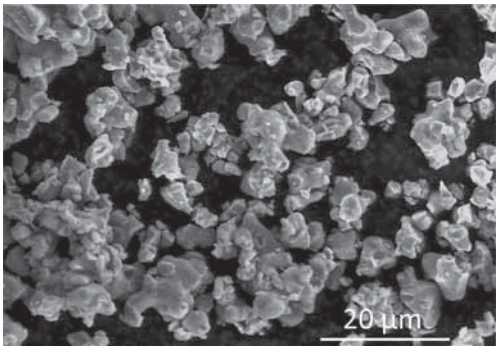

Figure 3. SEM image of BSCF powder.

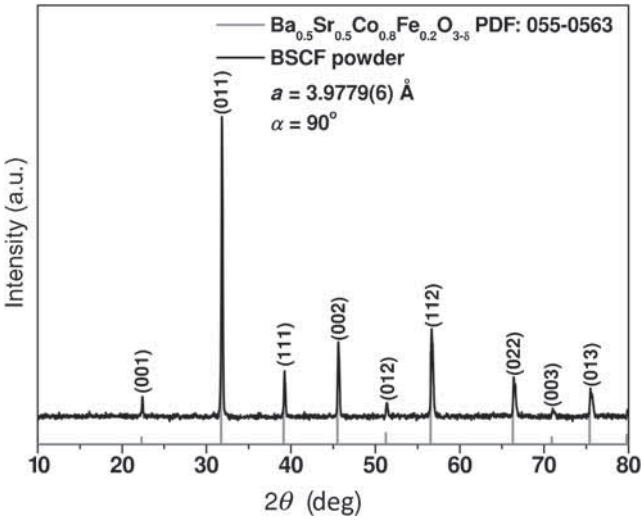

Figure 4. XRD pattern of BSCF powder.

3.2 *Rheological characterization of carriers and inks*

The flow curves for the two carriers (KF and KK) show that they have a quite different rheological behaviour (figure 5a, b). In the shear rate range investigated, the KF carrier is almost Newtonian with a slight decrease at high shear rates, while the KK carrier has a shear-thinning behaviour describable approximately by a power-law ($\eta = k\dot{\gamma}^{n-1}$) with slope

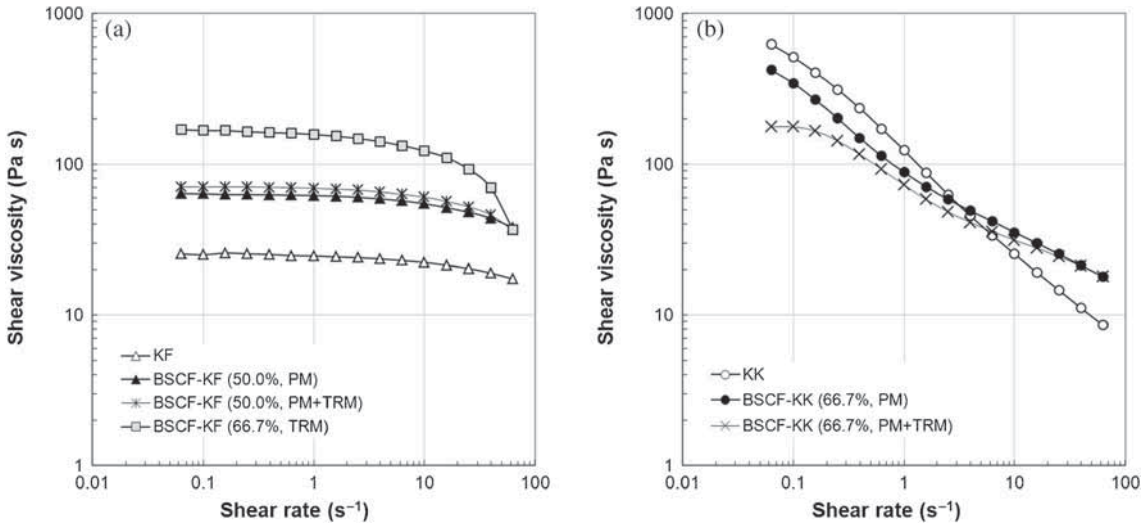

Figure 5. Flow curves for (**a**) KF- and (**b**) KK-based BSCF inks.

of about $n = 0.35$. This could be due to the presence of long polymeric chains of ethyl cellulose with higher molecular weight in the KK carrier. All the KF-based inks show a similar qualitative behaviour, regardless of the powder content or milling treatment (figure 5a). Introduction of 50 wt% of BSCF powder in the KF carrier increases the viscosity from about 25 to 63 Pa s. The curves corresponding to the two different treatments are very close showing that the three-rolls milling applied after the planetary milling does not affect significantly the ink behaviour. Assuming that the two milling treatments give comparable viscosities for any solid content, we can consider that the further increase of viscosity up to about 170 Pa recorded for the ink BSCF-KF (66.7%, TRM) is ascribable to the increase in the solid content from 50.0 to 66.7 wt%. However, for this ink, the decrease of viscosity at shear rates higher than 10 s^{-1} is much more pronounced than for the inks at 50% or for the carrier. Also in the case of the two KK-based inks, the effect of the three-rolls milling does not appear to be so significant even if at low shear rates, higher difference can be detected (figure 5b). It can be observed that while in the case of the KF-based inks, the TRM slightly increases the viscosity, for the KK-based inks such a treatment results in a viscosity decrease.

This opposite behaviour for the two families of inks can be observed also passing from the carrier to the ink, i.e., adding the powders to the carrier: while for the KF-inks such addition increases the viscosity, for the KK-inks, the viscosity decreases, at least at low shear rates. At higher shear rates, the flow curves for the KK-inks are almost overlapped and higher than the one of the KK carrier, as expected. It seems that the addition of the solid particles destroy the pre-existing structure of the KK carrier, as well the further treatment by three-rolls milling. Therefore, it can be supposed that the structure created by the polymeric chains of ethyl cellulose is very strong, but the powder destroys it, decreasing the viscosity. However, at high shear rates, when the structure has been completely breakdown by shearing, the presence of the particles makes the viscosity higher with respect to the carrier for mere hydrodynamic effects.

The levelling of the screen-printed layers of inks on the substrates and, therefore, the quality of printing, is affected also by the thixotropy of the inks. Thus, a specific test to highlight such phenomenon has been applied to the inks and compared with the behaviour of the carriers. In figure 6a and b, the shear stress recovery curves after sudden decreases in the flow conditions from a relatively high value (100 s^{-1}) are shown. The KF carrier (empty triangles in figure 6a) reaches immediately the shear stress corresponding to the equilibrium at the different shear rates applied, so that it is not thixotropic. At the lower shear rate applied (0.01 s^{-1}) the resulting torque is quite low (about $1.5 \cdot 10^{-6}$ Nm), close to the lower limit of the instrument, so that the sensitiveness are not good and the points are scattered. Instead, the KK carrier (empty circles in figure 6b) shows slight recovery of shear stress after the jumps indicating a low degree of thixotropy. As after each jump, both the carriers recover their shear stress value at 100 s^{-1}, they are not affected by irreversible effects.

Comparison with the corresponding inks shows that the BSCF-KK ink (filled circles) has qualitatively the same behaviour of the KK carrier (the shear stresses are only higher, except at 0.01 s^{-1}), while the BSCF-KF ink (filled triangles) is thixotropic with shear stress recoveries with time. From these results, it seems that the slight thixotropy of the KK-based ink is imposed by the carrier, while the more pronounced recoveries of the KF-based ink is not controlled by the carrier, but depends exclusively on the presence of BSCF powders. In other words, the thixotropic effect arising from the high content of powder in the KK-based ink is mitigated by the carrier probably due to the presence of the thixotropic agent, while in the KF-based inks, where such additive is not present, the thixotropy manifests itself. At 100 s^{-1} the behaviour of the BSCF-KF ink is probably affected by some flow instability, but the decrease of shear stress with time is quite clear and also reproducible after each jump.

The equilibrium states reached in each step of thixotropic test are in substantial agreement with the values obtained with the data collected during the return curve of the flow curves, except for the two carriers at 0.01 s^{-1} (instrument lower limit) and BSCF-KF ink at 100 s^{-1} (flow instabilities) (figure 7a, b).

The viscoelasticity of inks could affect the quality of the printing during the detachment of the screen from the support. Therefore, the determination of the viscoelastic properties could be useful to better design the inks, as well as to get information about their structuring. For the KF carrier, the elastic modulus G′ is lower than the viscous modulus G″ of roughly one order of magnitude and both change with frequency with a power law: $G' \propto \omega^{1.37}$, $G'' \propto \omega^{0.93}$. The viscous modulus of the KK carrier is almost overlapped with the one of the KF carrier, while the elastic one follows a different law (figure 8).

The introduction of BSCF powder in the KF carrier increases the values of the mechanical moduli, but the law of variation with the frequency remains the same (figure 9a, b). Instead, the introduction of the BSCF powders in the KK carrier reduces the elastic modulus (by keeping the same law of variation), while the viscous modulus is kept substantially unchanged (figure 9c, d). This is in agreement with the phenomenon observed for the flow curves. It seems that the introduction of the BSCF powder partially destroys the structure created by ethyl cellulose.

3.3 *SEM characterization of inks*

The five inks have been observed by SEM in low vacuum mode (figure 10a–e) and the images analysed by measuring about 350 particles and then stratified sampling as described above for the powder to get a particle size distribution after each milling condition. The milling treatments reduce the particle size with respect to dry powders and, in particular, the inks treated with three-rolls milling are finer with respect to the ones treated only with the planetary milling.

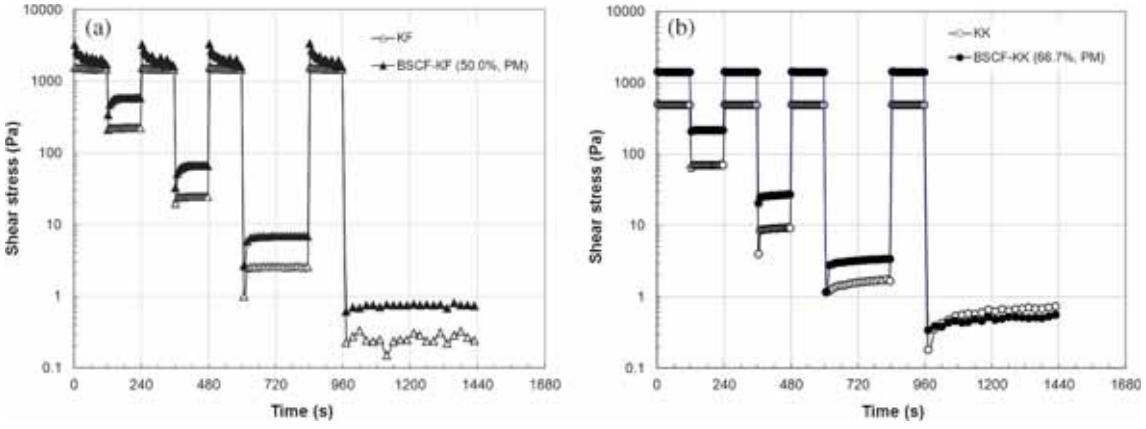

Figure 6. Shear stress changes at fixed shear rates for (**a**) KF- and (**b**) KK-based BSCF inks and carriers.

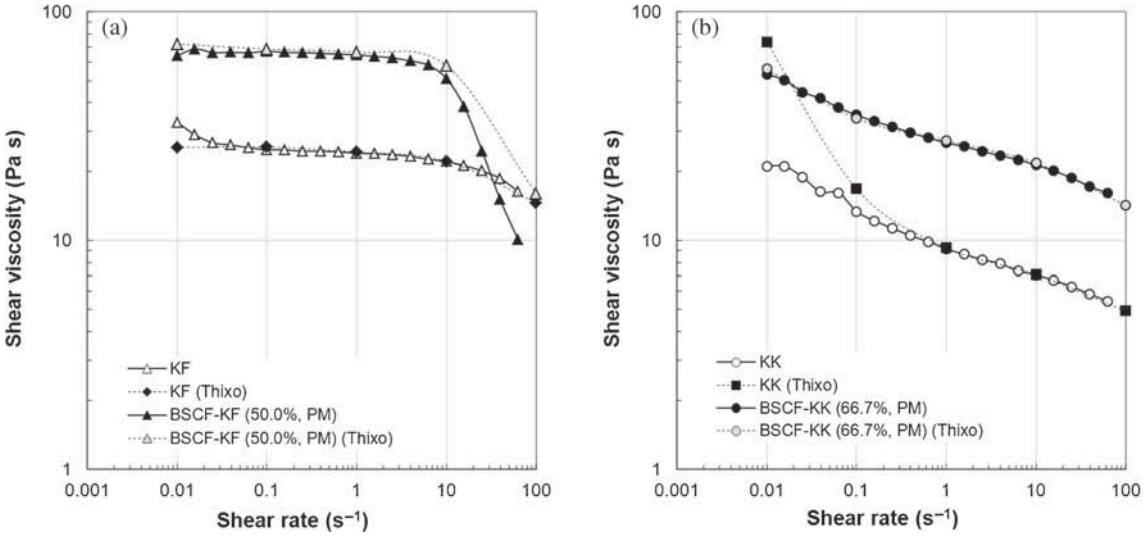

Figure 7. Comparison between flow curves and thixotropic tests for (**a**) KF- and (**b**) KK-based BSCF inks and carriers.

The KF-based ink treated only with the three-rolls milling is intermediate between the other two, much closer to the one treated with both the techniques. The KK-based inks are finer than the KF-based inks as demonstrated by the mean particle sizes of about 1 and 2 μm, respectively (figure 10f).

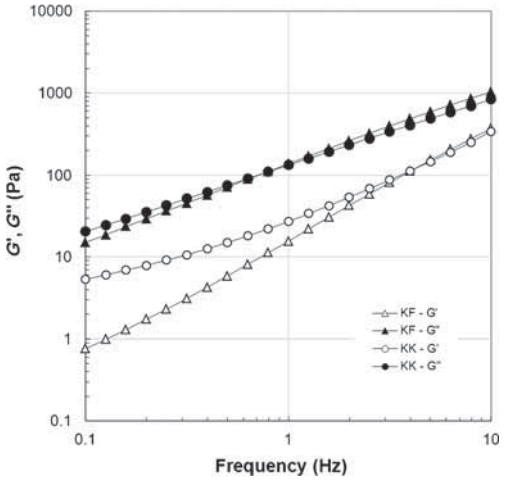

Figure 8. Comparison of mechanical spectra for KF and KK carriers.

3.4 *Microstructure of the sintered membranes*

After sintering at 1050°C of the first 30 samples, the resulted BSCF layers were well adhered to the porous supports. However, the sintering temperature of 1050°C resulted to be too low to make the perovskite layer fully-dense. Therefore, the other 30 samples were sintered at higher temperature (1150°C) with the same dwell time (5 h). The debinding cycle preceding the sintering was kept same for all the samples. From a visual inspection of the 60 samples, a statistics in relation with the quality of the layers was done (table 4). All the samples survived to the deposition/drying and sintering steps, except the ones made with the BSCF KF (66.7%, TRM) ink that were completely broken after sintering at 1050°C. Additionally, the density of BSCF layers after sintering (except for the broken samples) was verified using a red dye penetrant. The samples sintered at 1050°C have poor densities (the penetrant passed completely the thickness of the layer), as well as the 18 samples sintered at 1150°C and subjected to only planetary milling or three-rolls milling. Instead, the 12 samples that have undergone both the milling treatments (PM + TRM) showed a good density (the penetrant did not pass the layer).

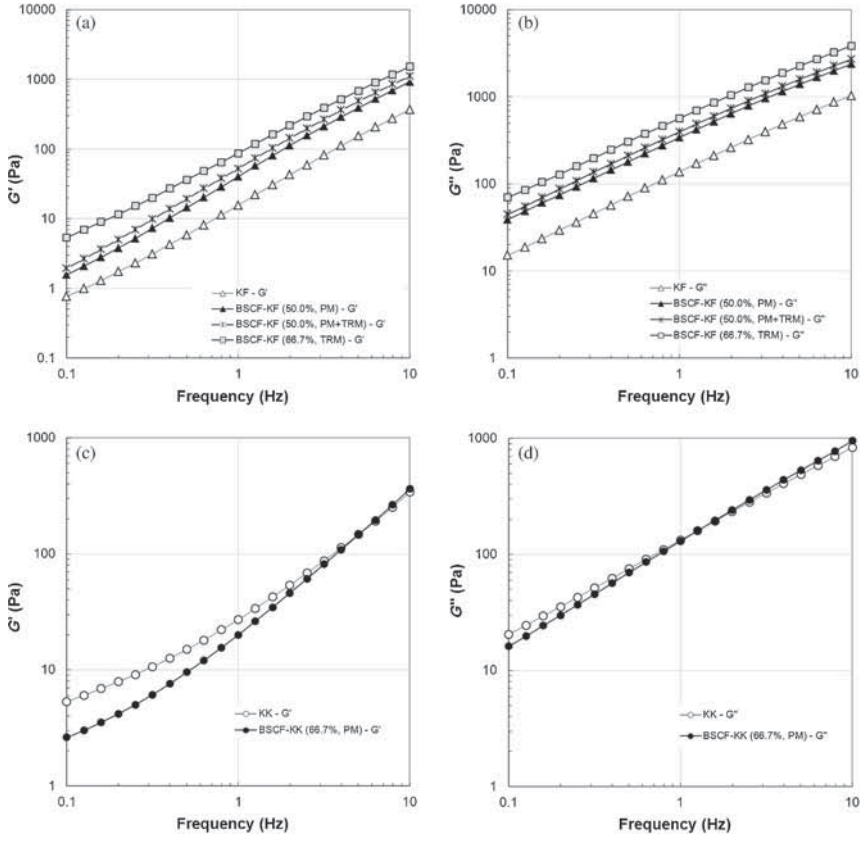

Figure 9. Mechanical moduli for KF-, (**a**) elastic and (**b**) viscous, and KK-based, (**c**) elastic and (**d**) viscous, BSCF inks and carriers.

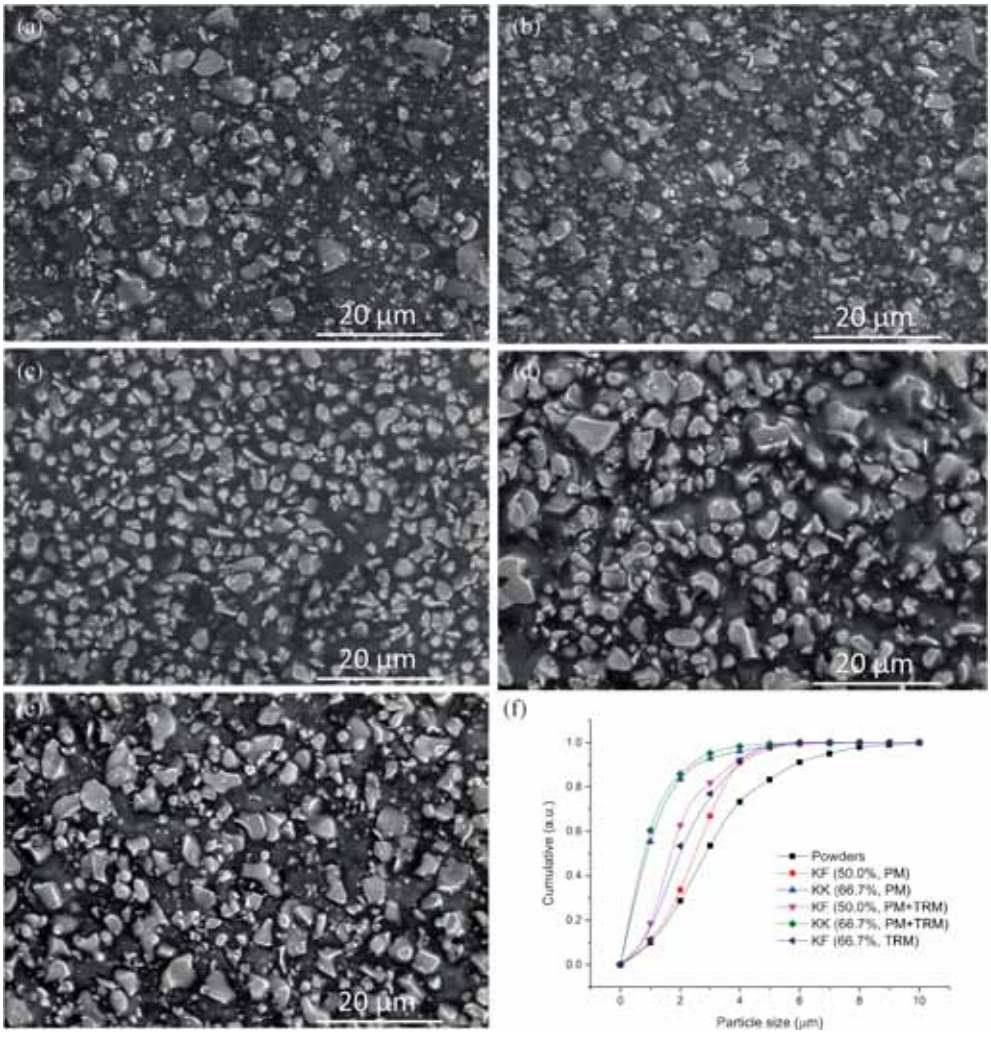

Figure 10. SEM images of BSCF inks: (**a**) KK (66.7%, PM), (**b**) KK (66.7%, PM+TRM), (**c**) KF (50.0%, PM), (**d**) KF (50.0%, PM+TRM), (**e**) KF (66.7%, TRM) and (**f**) particle size distribution for the inks and the powder.

Table 4. Results of visual inspection of the 60 samples.

Denotation	No. of successful samples after deposition /drying	Sintering temperature (°C)	No. of successful samples after sintering	Membrane density (by red dye penetrant)
BSCF KF (50.0%; PM)	12	1050	6	Poor
		1150	6	Poor
BSCF KK (66.7%; PM)	12	1050	6	Poor
		1150	6	Poor
BSCF KF (50.0%; PM + TRM)	12	1050	6	Poor
		1150	6	Good
BSCF KK (66.7%; PM + TRM)	12	1050	6	Poor
		1150	6	Good
BSCF KF (66.7%; TRM)	12	1050		N.D. (broken layer)
		1150	6	Poor

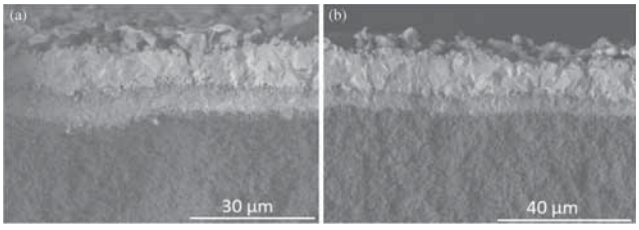

Figure 11. The fracture surface of (**a**) BSFC-KF (50.0%, PM + TRM) and (**b**) BSCF-KK (66.7%, PM + TRM) membranes sintered at 1150°C.

The microstructure of the layers for the samples with good density, BSCF-KF (50.0%, PM + TRM) and BSCF-KK (66.7%, PM + TRM) sintered at 1150°C, has been observed by SEM in high vacuum mode. From the fracture surfaces of both samples (figure 11a, b, respectively), an estimation of thickness of the layers was obtained, which ranges from 17 to 20 µm. Both samples are composed of three layers: the porous alumina support (at the bottom in the photos), an intermediate layer made of alumina and perovskite material with thickness of about 6 µm and finally the perovskite membrane (at the top in the photos). The photos show that there is a good adhesion among the layers and a fully dense membrane has been obtained upon heat treatment at 1150°C, even if a localized porosity at BSCF membrane/intermediate layer interface can be observed. The elemental analysis performed with the probe EDXS shows that a diffusion of aluminium from the substrate and barium, strontium and iron from the membrane occurred in opposite directions. The membrane layer is richer than barium, probably due to its lower diffusivity respect to the strontium and iron ions, and this would justify the lighter colour of that region. For cobalt, iron and strontium, the concentrations are similar to the stoichiometric ones.

4. Conclusions

Five BSCF inks were prepared using different formulations in terms of solid content (50, 66.7%) and carrier (KF, KK), and different milling treatments (PM, PM + TRM, TRM) were applied by screen printing to obtain thin dense BSCF membranes on three different porous alumina supports. The two carriers differ essentially for the different amount and nature of binder and for the addition in one of them of a thixotropy control agent. A thorough rheological characterization of the inks was performed and correlated to the composition and processing steps of the inks. The KK-based formulation characterized by a pseudoplastic and non-thixotropic behaviour seems to be the most promising as it lets to introduce the higher amount of powder (66.7 wt%) and results into a final highly dense membrane.

Acknowledgements

The activity was performed in the frame of the project SENERES—Sustainable Energy Research and Development Centre (FP7-REGPOT-2011-1) that supported the exchange of visits of the authors at ISTEC and CEREL.

References

[1] Teraoka Y, Nobunaga T and Yamazoe N 1988 *Chem. Lett.* 503
[2] McIntosh S, Vente J F, Haije W G, Blank D H A and Bouwmeester H J M 2006 *Chem. Mater.* **18** 2187
[3] Zhang C and Bristowe P D 2013 *RSC Advances* **3** 12267
[4] Baumann S, Serra J M, Lobera M P, Escolástico S, Schulze-Küppers F and Meulenberg W A 2011 *J. Membr. Sci.* **377** 198
[5] Jin W, Li S, Huang P, Xu N and Shi J 2001 *J. Membr. Sci.* **185** 237
[6] Li C, Hu T, Zhang H, Chen Y, Jin J and Yang N 2003 *J. Membr. Sci.* **226** 1
[7] Hong L, Chen X and Cao Z 2001 *J. Eur. Ceram. Soc.* **21** 2207
[8] Ramachandran D K, Clemens F, Glasscock A J, Søgaard M and Kaiser A 2014 *Ceram. Int.* **40** 10465
[9] Xing Y, Baumanna S, Uhlenbruck S, Rüttinger M, Venskutonis A, Meulenberg W A and Stöver D 2013 *J. Eur. Ceram. Soc.* **33** 287
[10] Somalu M R and Brandon N P 2012 *J. Am. Ceram. Soc.* **95** 1220
[11] Somalu M R, Yufit V and Brandon N P 2013 *Int. J. Hydrogen Energy* **38** 9500
[12] Ried P, Lorenz C, Brönstrup A, Graule T, Menzler N H, Sitte W and Holtappels P 2008 *J. Eur. Ceram. Soc.* **28** 1801
[13] Phair J W, Lundberg M and Kaiser A 2009 *Rheol. Acta* **48** 121
[14] Gromada M, Świder J, Trawczyński J, Stępień M and Wierzbicki M 2015 *Bull. Mater. Sci.* **38** 23